Received: October 6, 2022. Revised: November 24, 2022.

INASS

International Journal of
Intelligent Engineering & Systems

http://www.inass.org/

Intelligent Energy Management System Evaluation of Hybrid Electric Vehicle Based on Recurrent Wavelet Neural Network and PSO Algorithm

Mustafa A. Kamoona[1]* Omer Cihan Kivanc[1] Oday A Ahmed[2]

[1]*Department of Electrical and Electronics Engineering, Istanbul Okan University, Istanbul 34959, Turkey*
[2]*Department of Electrical Engineering, University of Technology, Baghdad, Iraq*
* Corresponding author's Email: mustafazzasim@gmail.com

Abstract: An energy management system (EMS) for hydrogen fuel cell hybrid electric vehicles (FCHEV) based on artificial intelligent (AI) technique is presented in this paper. In order to achieve a fast dynamic response and maintain high efficiency of energy storage resources, the fuzzy logic controller (FLC) and artificial neural networks (ANNs) are utilized for purpose of intelligently managing the system's power flow. Moreover, the feed-forward wavelet neural network linked with proportional-integral (PI) controller named (WNN-PI) and the recurrent wavelet neural network linked with PI controller named (RWNN-PI) are tuned by particle swarm optimization (PSO) algorithm, both are aimed at the operating of the resources at high efficiency with respect to their mechanism performance, meeting the load power demands efficiently, and reducing hydrogen usage. Finally, a comparison of the simulation outcomes is presented to choose the best of the proposed AI controllers where the results showed optimum power flow between power sources and load power of FCHEV then as consequence, the BAT and UC are run in a safe manner and extend their lifetime, also, the average efficiency of the FC stack has been increased, and the amount of usage of hydrogen fuel is reduced. The simulation of AI EMS has been carried out by MATLAB/Simulink R2022a, with various vehicle driving cycles by the advanced vehicle simulator (ADVISOR).

Keywords: Artificial intelligent, Recurrent wavelet neural network, EMS, PSO algorithm.

1. Introduction

Globally, with the intensification of technology and the globalization of the population, energy sources have become a need for everyday living. However, the dangers of this conventional energy exploitation have hardly ever been considered. For instance, the enormous number of automobiles in use globally has caused serious issues for the environment and people. Therefore, intensifying research for providing new approaches now to create energy sources that are less harmful to the environment, safer and more economical. Moreover, recently researchers and developers focused on reducing energy usage based on alternative vehicle technology.

Particularly, technology using fuel cells (FC) is regarded as an environmentally friendly energy source. Due to its longevity and environmentally benign emissions, it is regarded as green energy [1].

Transportation via fuel cell electric vehicles (FCEVs), fuel cell hybrid electric vehicles (FCHEVs) and battery electric vehicles (BEVs) have gained popularity. However, BEVs that use the battery pack as the main power has some drawbacks such as the short driving range [2], the battery requires hours to fully charge [3] and high cost and weight of BEVs due to their large battery packs [4]. Meanwhile, FCEVs have also some disadvantages such as dynamic response is slow as well as a high hydrogen cost, and the inability to recharge by the principle of regenerative braking energy [5].

The best solution to solve the drawbacks of both BEVs and FCEVs is to use a hybridization system of fuel cells (FC), batteries (B), and ultracapacitors (UC) in FCHEVs [6]. A developing successful energy management system is essential for controlling the power flow in order to use hydrogen

adequately and the auxiliary power sources efficiently respond to power demand [7,8]. The EMS uses artificial intelligence (AI) as well as an advanced controller for regulating the charge/discharge periods of the BAT and UC, ensuring optimal power flow between the energy resources within the efficient operation of the entire FCHEV, reducing the fuel consumption of the FC and also for expending lifetime of the FC, BAT and UC.

Numerous literary works addressed assessing and enhancing the performance of FCHEVs; the bulk tended to concentrate on EMSs. Moreover, optimization algorithms have attracted attention to EMS of hybrid electric vehicles and show outstanding features for improving the responses of EMS [10-12]. In [13] the authors present an online adaptive prognostics-based health management strategy for FCHEV; where the optimization problem has been developed for selecting the FLC parameters based on the state of charge (SOC) of the battery, the power demand, the fuel consumption as well as the fuel cell degradation. However, this strategy is rule-based and then able to produce a certified economy of fuel usage, but this does not ensure that it will attain the best optimal power flow. Also, even though GA is utilized in this method, it is not very adaptable, and the outcomes might change greatly under different driving situations.

Equivalent consumption minimization strategy (ECMS) is a control method for energy management of HEV as reported by [9]. This control minimizes energy consumption with consideration of the battery SOC, through the process of optimizing the torque split between the motor and engine. Moreover, ECMS can be implemented in adaptive or non-adaptive applications also being optimal control in terms of the cost function, for both battery aging, as well as fuel consumption by the Ah throughput method, is used to quantify battery aging. In general, it is feasible to find near-optimal solutions using ECMS. But since it identifies an optimum costate via repeated simulations, such approaches are problematic to apply to real applications. Also, the [14] presents the ECMS practical technique for predicting a suitable costate based on deep Q-networks (DQNs), a reinforcement learning algorithm that employs a deep neural network to assess performance and choose the best control parameter or costate. Although, the significant benefits of deep Q-networks, it is restricted because of an issue known as the "curse of dimensionality," which may happen because of the discretization of states and control variables.

The method used in [15] to regulate the flow of a hybrid system in response to variations in the load demand and battery SOC is the intelligent energy management system based on the adaptive neuro-fuzzy inference system ANFIS/Simulink toolbox. [16] conducted comparison results between FLC and ANFIS intelligent techniques to find out which sort of these intelligent systems should be employed for enhancing the SOC profile of the series-parallel plug-in hybrid electric vehicle. Overall, ANFIS can be applied and controlled within stable data, but it is challenging to control and work with load profiles that experience significant fluctuations, such as real vehicle driving cycles (e.g., UDDS, OCC or FTP).

Consequently, AI is used as advanced and accurate techniques in EMS over all kinds of EVs, including wavelet strategies. Whereby, [17] presents a frequency decoupling-based energy management strategy (EMS) for electrical hybrid vehicles with fuel cells, batteries, and ultracapacitors (FCHEV) by employing fuzzy control approach. This method decomposes the frequency into three ranges by using Harr wavelet transform and an adaptive-fuzzy filter. Resulting in, increase fuel efficiency, prolonged fuel cell lifespan as well a 7.94% decrease in fuel consumption over the ECMS. [18] reported a real-time predictive energy management technique for the FCHEV. In order to forecast future velocity, an LSTM neural network is proposed, and based on that the wavelet transform algorithm is utilized.

Authors in [23] present a wavelet neural network parallel with PID controller as dynamic and recurrent dynamic methods (DWNN-PID and RDWNN-PID) tuned by PSO algorithm for controlling the speed of BLDC motor with a comparative study where results that the DWNN-PID is more efficient than other controllers.

This paper's key objective is to implement intelligent EMS for FCHEV. Where the proposed architecture of plug-in FCHEV, combines FC PEMFC type as the main power source with the BAT and UC as secondary power sources with a controller that works under any driving cycles. Overall, the major contributions of this work are listed below:

- Involves AI EMS by FLC and ANNs for controlling the FC converter and advanced controller for controlling the BAT converter by using wavelet neural networks as feed-forward method (WNN-PI) and recurrent method of wavelet neural network (RWNN-PI), for regulating the charge/discharge periods of the BAT and UC, and also ensure optimal power flow between the energy resources within the

effective operation of overall FCHEV system.

- Maintain the 300 volts as the set desired level of the DC-bus voltage.
- Verify that the supplying for switching converters of the FC and BAT is with appropriate signals to guarantee that the hybrid FC system responds to entire load dynamics.
- The suggested design is tested across three vehicle driving cycles to see how reliable it is when used with various drive cycles.
- The FC, BAT, and UC are modeled based on their manufacturer datasheets. As a consequence, the properties of the power sources have thus been obtained as close to their real characteristics.
- Providing a comparative outcomes study to choose the best among these AI controllers.
- Providing a PSO algorithm that could use to tune many different parameters of applications controller.

The remainder of this paper is organized as follows. Section 2 presents the FCHEV architecture, power sources model and strategy of power flow. Section 3 illustrates the description of intelligent control for the FC and BAT converters. In section 4 simulation results and discussions of all proposed controllers. Finally, the conclusion of the intelligent EMS is presented in section 5.

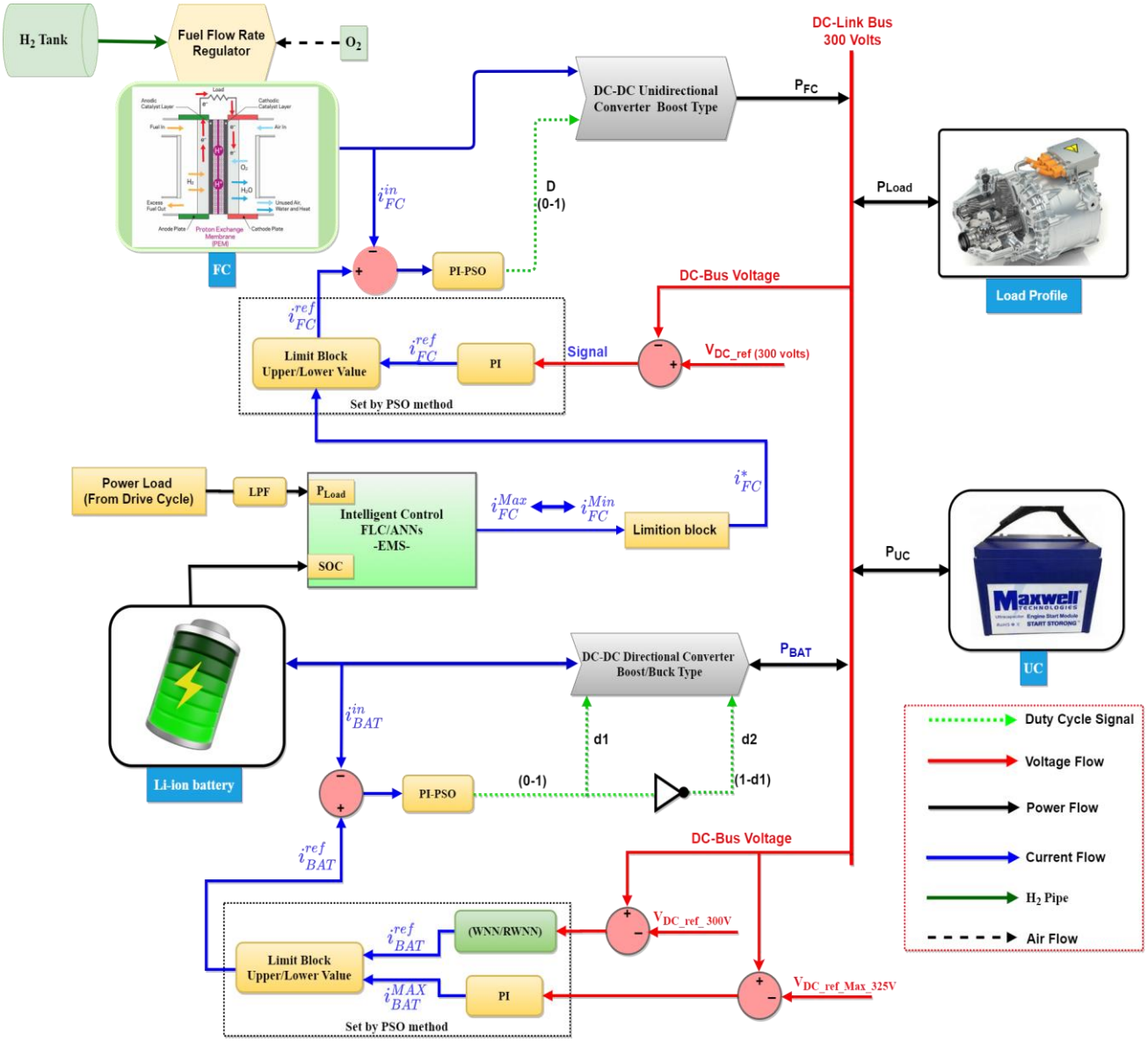

Figure. 1 The developed plug-in FCHEV configuration of the proposed EMS

2. Methodology

2.1 Architecture of the proposed FCHEV

The configurations of FCHEV are divided into three categories which are: Active, semi-active and passive [6]. The proposed topology architecture is semi-active, hence structured as the UC is linked directly to the DC-bus without a converter, the FC is connected to the DC-bus via a unidirectional DC-DC converter and a bidirectional DC-DC converter connects BAT to the DC-bus.

Fig. 1 shows the block diagram of the proposed topology with the main control diagram. The boost/buck converter is set to be controlling the BAT output voltage. Hence, step up/down the voltage of BAT in order to keep the DC-bus at 300 volts. BAT converter is bidirectional which able to invest the power of sudden braking to recharge the BAT but first, the UC is recharged before the BAT due to the UC features that respond quickly to rapid changes in power demands [19]; BAT converter controlled by wavelet strategies parallel with PI controllers which are named (WNN-PI and RWNN-PI) both are tunning online by POS algorithm. While the FC converter is a boost type which controlled by EMS that has one of two controllers (FLC or ANNs). Overall, the control structure is objective at covering the desired power load of the vehicle efficiently which yields the best control over hydrogen consumption, improvements in the FC responsiveness and efficiency of FC runs, an extension of the FC and BAT lifespan, and a reduction in the size of the FC stack system, which in turn lowers the FC cost. The main block diagram of the controller EMS strategy is shown above, which extremely demonstrates that converters are controlled by the reference duty cycle. In order to find the reference duty cycles, an AI controller is required for obtaining the system reference values and adjust the system to the desired value under an optimal power flow of the FCHEV. Due to the vehicle's abrupt acceleration and deceleration, a Low Pass Filter (LPF) has been utilized to reduce the load profile high frequencies.

2.2 Power sources model parameters

Our proposed FCHEV model intended to establish the power sources with the same properties as their manufacturer datasheets, which in turn made the Simulink "SimPowerSystem" model of power sources accurate and as same as their actual qualities.

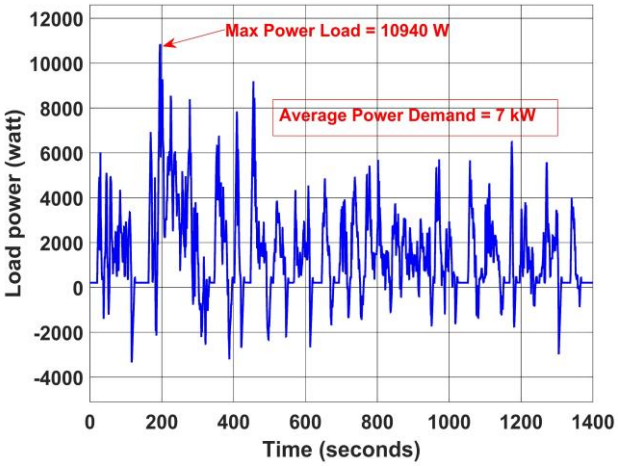

Figure. 2 Power profile of the UDDS

Thus, the performance results of the system are realistic as possible in the real world. Moreover, the power sources (FC, UC, and BAT) are designed based on the load profile. In order to assess the design, three drive cycles have been employed. Urban-dynamometer-driving-schedule (UDDS), orange county bus cycle (OCC) and federal test procedure (FTP), these drive cycles are captured by the ADVISOR analysis program. The basic driving cycle used is UDDS for analysing FCHEV performance since has the greatest variations in peak power usage compared to the other driving cycle standards. Therefore, the proposed FCHEV is able to function under different driving cycles. Consequently, guarantees that the proposed intelligent EMS is a trustworthy and predictable system. Fig. 2 illustrates the UDDS power profile.

The maximum power load for UDDS, as seen in Fig. 2, is 10.940kW, assuming that the maximum power load is approximate 11kW delivered over a time span of 1400 seconds. As a result, the power requirements of the FC, BAT, and UC have been created to handle the entire load. Models for power sources were created by using their datasheets (UC [20], BAT [21] and FC [22]):

- Ultracapacitor: The type is Maxwell 1200F, 2.7V/cell Boostcap®BCAP1200 UC. DC-bus of the proposed FCHEV is 300 volts and as the structure that UC connected directly to DC-bus then UC should have 300 volts output voltage. Therefore, 1200F, 2.7V/cell use 120 connected in series (n cells) which is able to produce 11kW in 10 seconds.
- Battery: The type is Valence Technology U-Charge U1-12XP lithium-ion BAT. Four cells are connected in series. The nominal voltage of each series is 12.6V, then a 48V is easily

reached without going above the converter duty cycle's stable dynamic range. 40Ah is the maximum capacity of BAT. As a consequence, the battery system can deliver 4.937kW.

- Fuel cell: The type is Hydrogenics 12.5kW HyPM-HD12 PEMFC. Used 65 cells; FC converter efficiency is considered to be 88%. As a consequence, the FC is capable of supplying around 7.95kW, which is sufficient to meet the average power load of 7kW.

2.3 Optimal power flow strategy rules

The following factors need to be taken into account in order to regulate the output power of the FC and fulfil all of the FCHEV's operational requirements in terms of power flow. Expressed the maximum fuel cell power as (P_{fc_max}) = 9kW, optimal fuel cell power as (P_{fc_opt}) = 1.6kW and minimum fuel cell power as (P_{fc_min}) = 0.5kW. Table 1 shows the rules of optimizes the power flow under three modes of (BAT_{SOC}). As mentioned in Fig. 1 the EMS has two inputs which are the power of FC (Pfc) and the state of charge for the battery (BATSOC). To get the reference current for feeding the FC boost converter by developing controllers, EMS fulfils the output power of the FC. This optimizes the power flow and prevents abrupt changes in the load power on the FC and BAT.

Table 1. Optimal power flow rules

BAT_{SOC} is lower than 65%		
IF the P_{load}	P_{fc} to Load By	BAT&UC States
$P_{load} > P_{fc\_max}$	P_{fc_max}	UC Discharging
$P_{fc\_max} < P_{load} > P_{fc\_opt}$	P_{fc_max}	------
$P_{fc\_opt} < P_{load} > P_{fc\_min}$	P_{fc_opt}	BAT Charging
$P_{fc\_min} < P_{load} > 0$	P_{fc_min}	BAT Charging
Braking mode ($-P_{load}$)	------	BAT Charging by (P_{fc_opt})+($-P_{load}$)
BAT_{SOC} is between 60% and 85%		
$P_{load} > P_{fc\_max}$	P_{fc_max}	BAT&UC Discharging
$P_{fc\_max} < P_{load} > P_{fc\_opt}$	P_{fc_max}	------
$P_{fc\_opt} < P_{load} > 0$	P_{fc_opt}	BAT Charging
Braking mode ($-P_{load}$)	------	BAT Charging by (P_{fc_min})+($-P_{load}$)
BAT_{SOC} is above 85%		
$P_{load} > P_{fc\_max}$	P_{fc_max}	BAT&UC Discharging
$P_{fc\_max} < P_{load} > P_{fc\_opt}$	P_{fc_max}	------
$P_{fc\_opt} < P_{load} > 0$	P_{fc_min}	BAT Discharging
Braking mode ($-P_{load}$)	------	BAT&UC Charging by ($-P_{load}$)

Algorithm 1: Generate ANNs by MATLAB Code

```
Step.1:  Initialize Net Type "feedforwardnet"
           No. of hidden layers
             Neurons of each layer
code  >  Net=feedforwardnet([30 20 15 10]);
Step.2:  divide data
           70% for t training
             15% for testing,
               15% for validation
code  >  Net.divideParam.trainRatio=0.7;
         Net.divideParam.testRatio=0.15;
         Net.divideParam.valRatio=0.15;
Step.3:  Set Learning Rate=0.001
code  >  Net.trainParam.lr=0.001;
Step.4:  Set Performance and Gradient goal
code  >  Net.trainParam.min_grad=1e-20;
         Net.trainParam.goal=1e-30;
Step.5:  No. of epochs = 1000
code  >  Net.trainParam.epochs=1000;
Step.6:  train Net by Input/output data of FLC
code  >  Net=train(Net,inputdata,outpudata)
Step.7:  Export Net to the Simulink Environment
code  >  gensim(Net)
```

3. Intelligent control system models for FC and BAT converters

The BAT and FC current boundaries are determined and controlled by the proposed controllers (PI-PSO, WNN-PI, RWNN-PI, and the developed (EMS by FLC and ANNs)), in order to guarantee the proper times for the charge and discharge of the BAT/UC and no reverse current feed to the FC. The (i_{FC}^{*}) is send to a single-quadrature converter since the FC only responds to steady-state load power, whereas the (i_{BAT}^{ref}) of the BAT is fed to a two-quadrature converter.

4. Intelligent control system models for FC and BAT converters

The BAT and FC current boundaries are determined and controlled by the proposed controllers (PI-PSO, WNN-PI, RWNN-PI, and the developed (EMS by FLC and ANNs)), in order to guarantee the proper times for the charge and

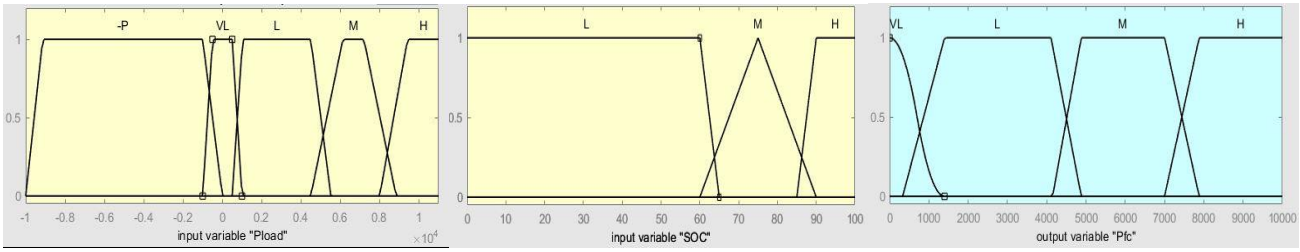

(a) (b) (c)

Figure. 3 FLC membership (a) is load power, (b) is BAT state of charge and (c) is the FC output power reference

Table 2. FLC rules

Input	IF (P_{Load})	H	M	L	VL	-P	H	M	L	VL	-P	H	M	L	VL	-P
	AND (BAT_{SOC})	H	H	H	H	H	M	M	M	M	M	L	L	L	L	L
Output	THEN (P_{fc})	H	M	L	VL	VL	H	M	L	VL	VL	H	H	M	L	L

discharge of the BAT/UC and no reverse current feed to the FC. The (i_{FC}^{*}) is send to a single-quadrature converter since the FC only responds to steady-state load power, whereas the (i_{BAT}^{ref}) of the BAT is fed to a two-quadrature converter.

4.1 Architecture FLC of FC converter

The output of the EMS-FLC is the FC reference power (Pfc). Inputs include (BAT_{SOC}) and (PLoad). A set of if-then rules based on the Table 1 rules have been utilized in FLC membership functions. A trapezoidal membership function (trapmf) is utilized to create FLC, and Mamdani's fuzzy inference approach is employed for defuzzification, as illustrated in Fig. 3 the developed FLC membership. Table 2 shows the FLC rules.
Where: H = high, M = medium, L = low, VL = very low and -P = negative power.

4.2 Architecture ANNs of FC converter

For training, the ANNs require input and output data. Therefore, the EMS has been developed by using the FLC scheme first in order to collect the necessary input/output data.

The following are the parameters of the ANNs for EMS: The training technique is "Levenberg-Marquardt" and the network used is "feedforwardnet." Four hidden layers have been employed, with the neurons of each layer being (30, 20, 15, 10). The training target error (MSE) is 10^{-30}. 15% for testing, 15% for validation, and 70% of the data for training. Algorithm 1 shows the procedure of building the ANNs by MATLAB script codes.

4.3 Architecture WNN of BAT converter

By comparing the difference between the DC link voltage signal (V_Actual) and the DC-bus reference voltage signal (V_{DC_ref}), the wavelet linked with PI controller attempts to manage the current boundary of the BAT that is based on the (i_{BAT}^{max}). In order to adjust the translation parameters of the connection weights in the WNN (a's, b's, w's) and the parameter (kp & ki) of the PI controller online using the Simulink model of hybrid FCEV, the Recurrent and Feed-forward wavelet neural network are utilized with the PSO learning method. Also, using a PI controller optimized by using PSO to obtain the (i_{BAT}^{max}). The PSO method uses the Integral of Squared Error (ISE) criteria and the overshoot (Mp) criterion to figure out the cost fitness for an optimal value.

$$fitness\ function = \min(ISE) + \min(Mp) \quad (1)$$

$$\mathrm{ISE} = \int \mathrm{e}^2(\mathrm{t})\mathrm{dt} \quad (2)$$

$$\mathrm{M_p} = \max(\mathrm{V}) - (\mathrm{V_{ref}}) \quad (3)$$

$$e(i) = \mathrm{D(i)} - \mathrm{y(i)} \quad (4)$$

Where e(i) is the error that can be obtained by subtracting the wanted value D(i) from the actual value of the model y(i). Where V is the measured voltage and V_{ref} is the reference value (300 volts). Then, each swarm particle's current location x i (t) and speed v i (t) should be keep updating by using Eq. (5):

$$\mathrm{v_i^{k+1}} = \mathrm{w} * \mathrm{v_i^k} + \mathrm{c_1} * \mathrm{R_1} * \left(\mathrm{lbest_i} - \mathrm{x_i^k}\right) + \mathrm{c_2} * \mathrm{R_2} * \left(\mathrm{gbest_i} - \mathrm{x_i^k}\right) \quad (5)$$

Adjusting the current position by Eq. (6):

$$x_i^{k+1} = x_i^k + v_i^{k+1} \quad (6)$$

A group of daughter wavelets are combined linearly, the result is a generalized wavelet $\psi_{a,b}$:

$$\psi_{a,b} = \psi\left(\frac{x-b}{a}\right) \quad (7)$$

Then final output of the wavelet is:

$$y = \sum_{n=1}^{N} w_N \psi_{a_N,b_N} \quad (8)$$

As shown in Fig. 1 after comparing these currents which are processed by the PI-PSO controller to modify the d1 and d2 of the BAT converter's power switching signal. The proposed RWNN-PI is known as "partially feedback". Where comprises three layers: the hidden layer has four neurons, the input layer has two inputs and the output layer has one output as shown in Fig. 4. While the WNN-PI is same as the RWNN-PI structure except the neurons is eight and without feedback signal. Both are aimed to find (i_{BAT}^{ref}). Algorithm 2 shows the PSO steps for finding the wavelet and PI parameters by MATLAB script codes.

Algorithm 2: PSO to find optimum values for (WNN/RWNN) and PI parameters.

Initialization PSO
No. of birds ***n= 15***, *No.* ***birds_steps =15***
Dimension of the problem (dim)
Step.1: *for WNN-PI = 26 RWNN-PI = 14*
PSO parameters ***c1 & c2 = 1.4***
Inertia ***w =0.8***
> ***fitness=0*ones(n,bird_setp);***
Initialize the parameter
Step.2: *R1 & R2 = rand(n,dim);*
> ***current_fitness =0*ones(n,1);***
Step.3: *Initializing swarm and velocities and position*
current_position = abs(10*(rand(n,dim)-.5));
> ***velocity = .3*randn(n,dim);***
local_best_position = current_position;
Step.4: *Evaluate initial population*
> ***for i = 1:n***
PI=current_position(i,:);
Step.5: *Set all (a's, b's, w's) and (kp & ki)*
b_{1-4} = PI($_{1-4}$); *and same for a's, w's and (kp & ki)*
Initialize sim options (Simulink)
simopt=simset('solver','ode45','SrcWorkspace','Current','DstWorkspace','Current');
[tout,xout,yout]=sim('mutatafaRWNN',[0 1400],simopt); *% 1400 sec. is UDDS*
Compute the error
sys_overshoot=max(V_Actual)-300;
m=abs(e);
error=sum(m);
F=error+sys_overshoot;
current_fitness(i)=F;
end
Velocity Update
Step.6: > ***velocity = w *velocity + c1*(R1.*(local_best_position-current_position))+c2*(R2.*(globl_best_position-current_position));***
Step.7: *Swarm Update*
Step.8: *Evaluate anew swarm: Back to Step.5:*
Step.9: *Select the optimum values and send them to Simulink.*
> ***b_{1-4} = globl_best_position(n,$_{1-4}$);***
Same for a's, w's and (kp & ki)

Table 3. RWNN parameters tuned using PSO

RWNN Dilation parameters		RWNN Translation parameters		RWNN Weights parameters	
a1	11.0776	b1	-0.7579	w1	14.7592
a2	-21.9609	b2	0.4560	w2	11.2434
a3	6.8087	b3	7.8331	w3	-0.1116
a4	13.3339	b4	3.9727	w4	29.1614

Outcomes of the proposed PSO algorithm after running the model (n= 15, No. birds_steps =15 so 225 times run are fulfilled). The optimal values for the PI controller parameters are (kp = 25.9874 & ki = 1.1762) and the RWNN parameters (a's, b's, w's) are listed in Table 3.

5. Simulation results and discussions

This section shows the simulation results for AI EMS that is evaluated under three drive cycles UDDS, OCC and FTP via three control methodologies (CMs) which are named:

1- Control methodology-1 (CM-1): FC by FLC and BAT by feed-forward wavelet neural network (WNN-PI).

2- Control methodology-2 (CM-2): FC by ANNs and BAT by feed-forward wavelet neural network (WNN-PI).
3- Control methodology-3 (CM-3): FC by ANNs and BAT via recurrent wavelet neural network (RWNN-PI).

The AI EMS has been evaluated by (CM-1) during UDDS first then the input and output data of the FLC scheme has been used to train the proposed ANNs to see its performance under different drive cycles (OCC and FTP). It is noted that the results of the FLC and ANNs at UDDS are very close due to the ANNs trained on the same drive cycle (UDDS) and because the trained network is well trained and a small mean square error was attained.

The DC voltage bus fluctuation due to the changes in the load power demand as shown in Fig. 5 the DC-bus voltage under UDDS. Whereas all the proposed control methodologies have limited the DC-bus; which are adjust the voltage of the DC link at the reference level (300 volts). The (CM-1, CM-2 and CM-3) successfully kept the DC-bus at an acceptable level since the designed DC-bus voltage level is set between 290 to 320V. But, the (CM-3) keeps DC-bus to the nearest level of 300 volts more than (CM-1 and CM-2); where DC-bus by (CM-3) is between 295.9V-305.2V (Mean value is 301V), and DC-bus by (CM-1 and CM-2) is between 295.88V-306.3V (Mean value is 301.7V), and between 295.2V-307.2V (Mean value is 301.8V) respectively.

The suggested control techniques (CM-1, CM-2 and CM-3) effectively satisfy the AI EMS of FCHEV's requirements during the UDDS and successfully meet the rules of Table 1 for charging/recharging the BAT and UC. Hence, FC power is steady-state under load power demand and without responding to sudden load changes; the BAT provides a medium-frequency component to the load power demand which led to assists the FC to cover the remaining load power required; the UC power is delivering the high-frequency components to load power demand for handling rapid load changes as shown in Fig. 6 the delivering power of the resources (FC, BAT and UC) during UDDS by CM-3. Overall, optimum power flow achieved of FCHEV which in return the BAT and UC are run in a safe manner and extend their lifetime, as well as, reducing the H_2 (Hydrogen) usage. While the FC power under OCC and FTP drive cycles has overshot as shown in Fig. 7 the FC power under the OCC drive cycle there is overshooting once reaches over the second 1400 because the FLC of CM-1 is designed according to UDDS, therefore faced this problem at the cycles OCC and FTP, but the CM-3 is successfully running the FC under the different drive cycles without any overshot as shown in Fig. 8 and Fig. 9 the FC power under OCC and FTP effectively, during the whole cycle pried time 2500

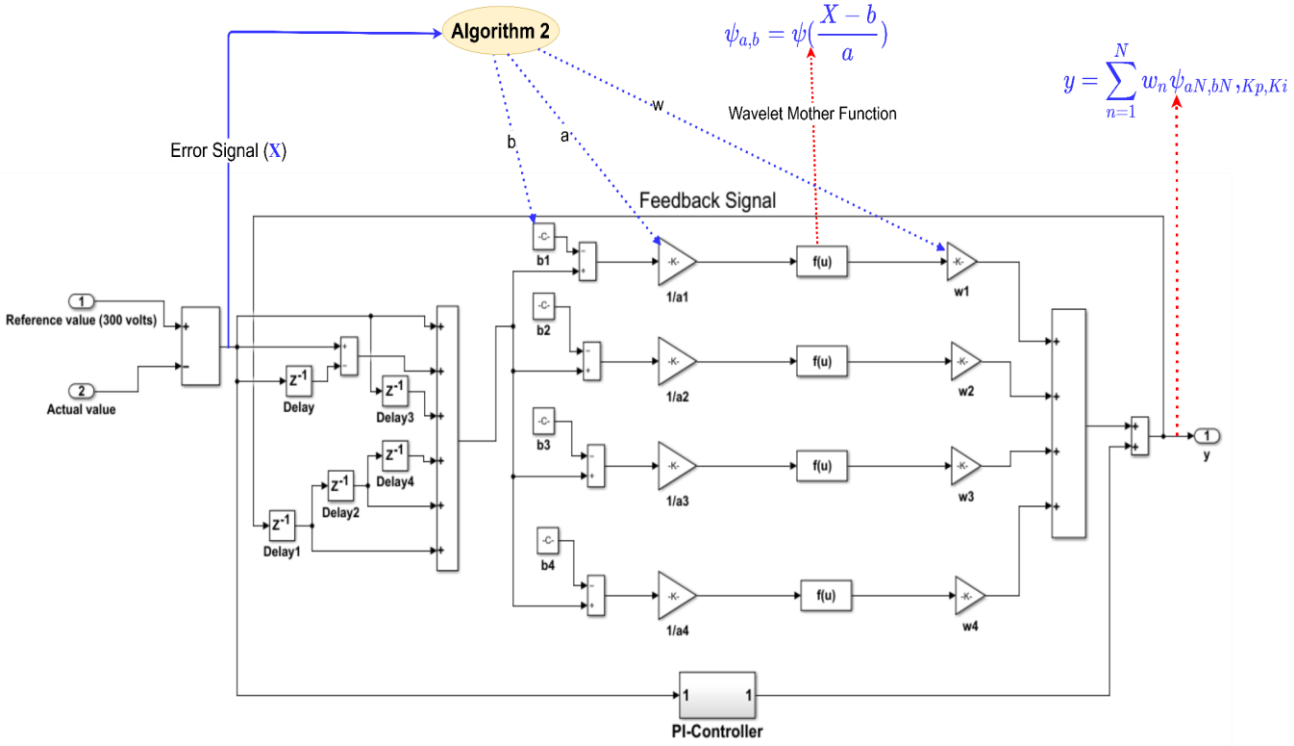

Figure. 4 RWNN-PI structure tuned by PSO

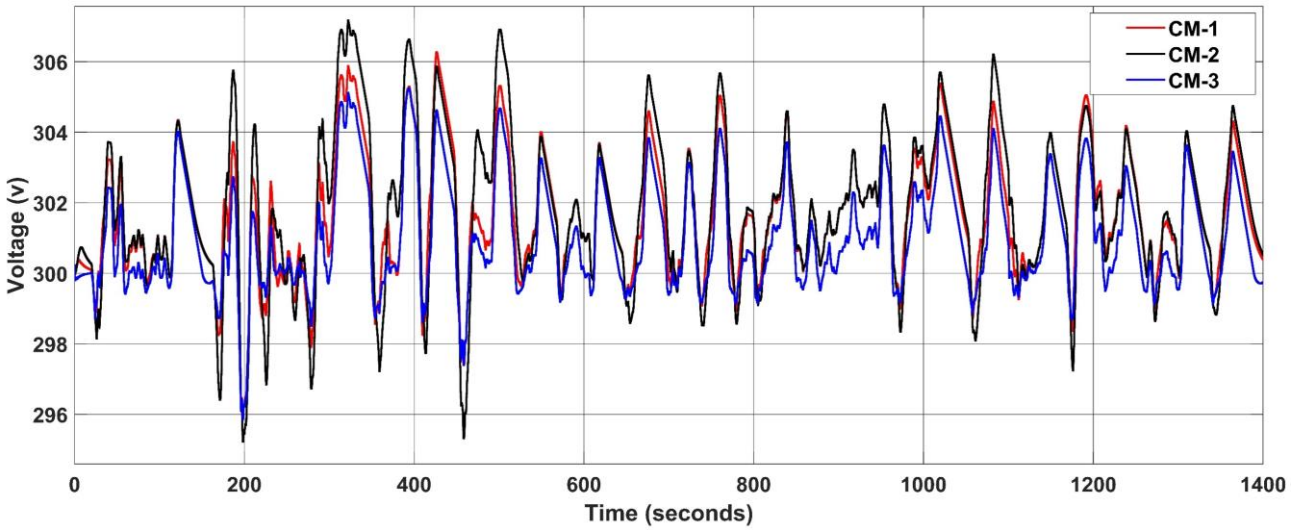

Figure. 5 DC-bus under UDDS load

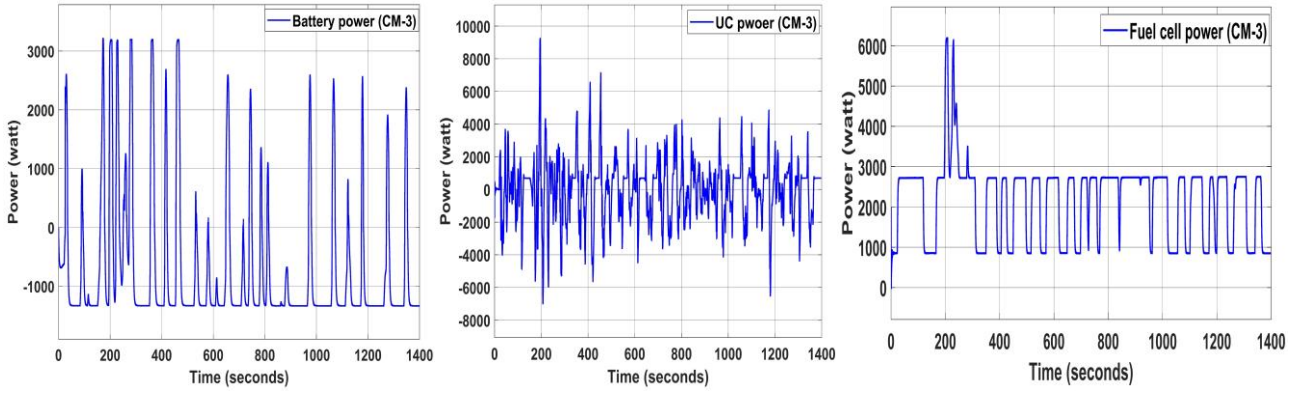

(a) (b) (c)

Figure. 6 Power delivered by the sources during UDDS (a) BAT power, (b) UC power and (c) FC power

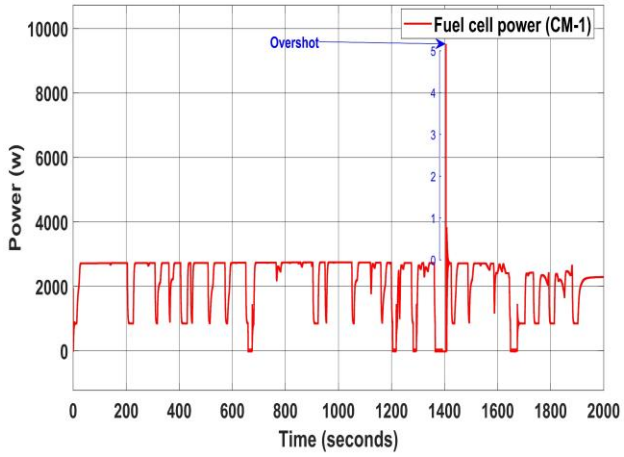

Figure. 7 FC power during OCC

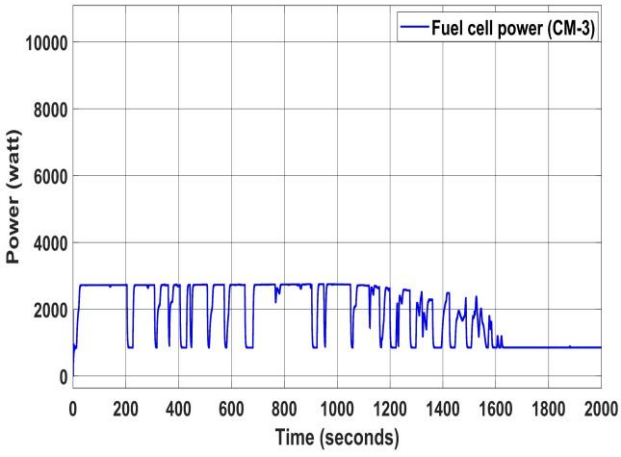

Figure. 8 FC power during OCC

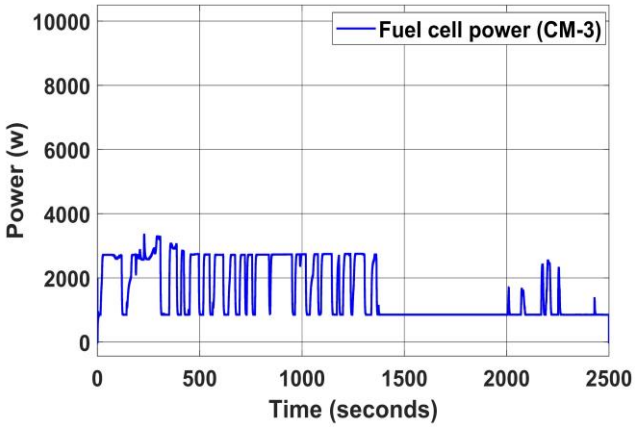

Figure. 9 FC power during FTP

seconds of the FTP observed no overshot. This is because the ANNs is a predictable system and the RWNN-PI is more efficient than WNN-PI.

Moreover, the duty cycle values of the converters are acceptable whereby all are not above 90% by the proposed control methodologies. However, the duty cycles by CM-3 are more efficient and stable than (CM-1) as shown in Fig. 10.

The designed AI EMS which is based on the three control methodologies is maintained the SOC for both BAT and UC as described in Table 1, where the SOC set to be between (60%-85%). Hence, the SOC for the BAT is between (67.1%-74.82%) and UC is between (83.26%-86.84%) during UDDS which are controlled by (CM-3) as shown in Fig. 11. AI EMS strives to guarantee that the BAT and UC have sufficient charge for the FCHEV acceleration periods. Meanwhile, reducing H2 use by optimizing the energy flow between the resources power and the load power demand.

According to Fig. 11, it is clearly observed that the UC has the fastest response; in terms of charging and discharging. Consequently, the FC and BAT voltage are under their desired region, the FC voltage range is between (43.74V-49.44V) as shown in Fig. 12 also BAT voltage is stable and within a small range between 50.15V and 52.69V without endangering the BAT to discharge or charge excessively as shown in Fig. 13.

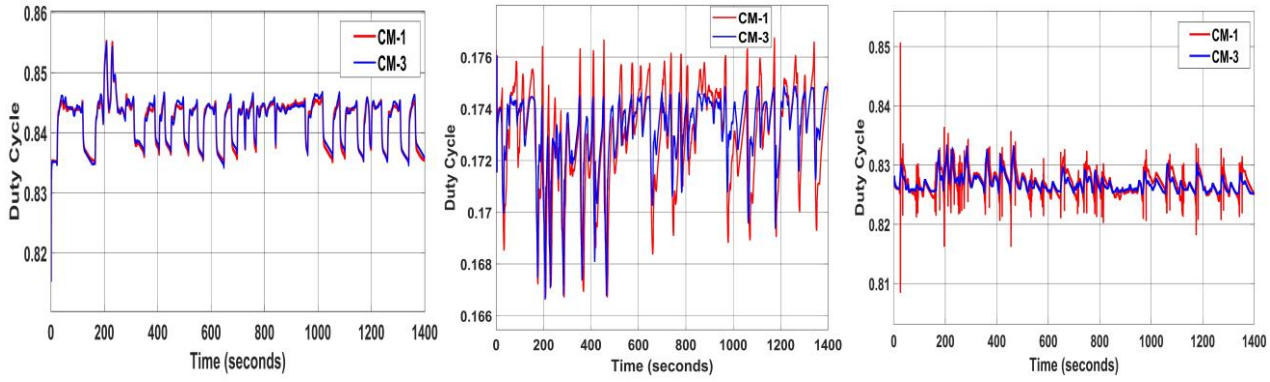

(a) (b) (c)

Figure. 10 Converters duty cycle during UDDS (a) FC boost cycle, (b) BAT buck cycle and (c) BAT boost cycle

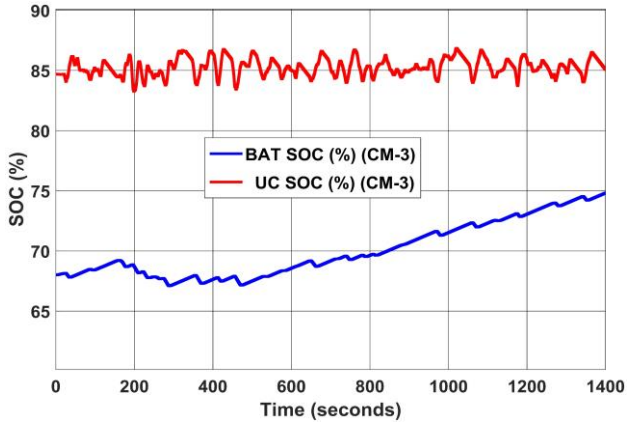

Figure. 11 The SOC (%) of BAT and UC during UDDS

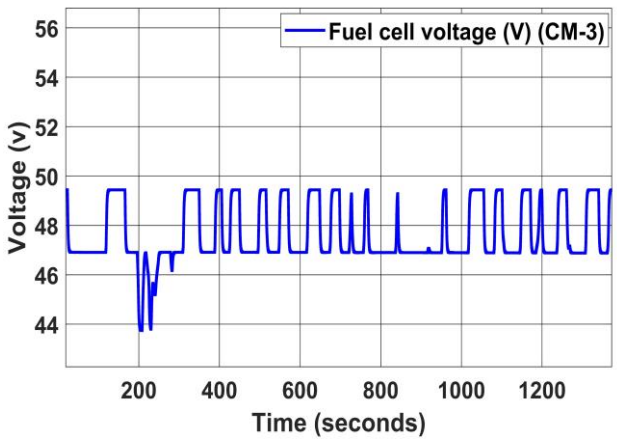

Figure. 12 FC voltage during UDDS

Overall, CM-3 efficiently reduces fuel consumption utilization, which leads to an improvement in FC stack efficiency. Fig. 14 shows the H_2 fuel consumption (lpm). The FC stack efficiency during UDDS, which is managed by CM-3, is shown in Fig. 15. In addition, Table 4 depicts the average FC stack efficiency and mean value of H_2 fuel consumption (lpm) throughout the three driving cycles in comparison to the proposed control approaches (CM-1, CM-2 and CM-3).

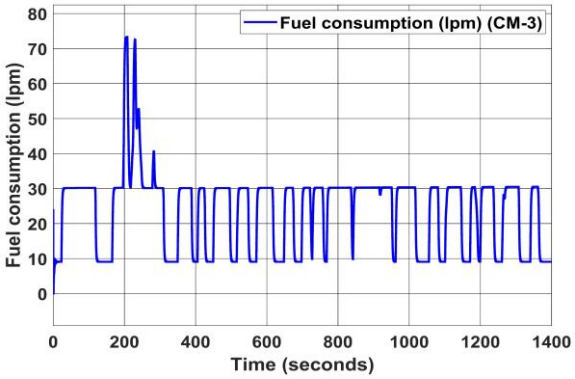

Figure. 14 H2 fuel consumption during UDDS

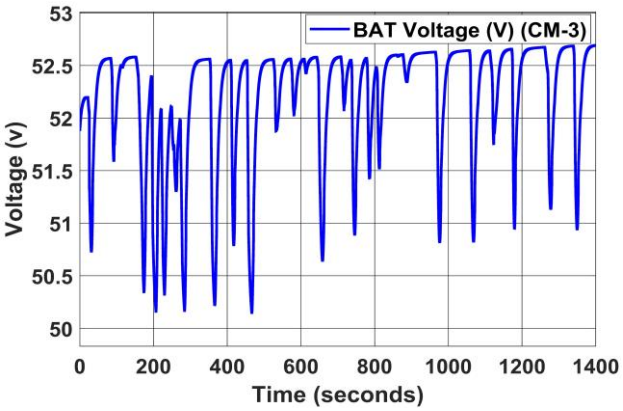

Figure. 13 BAT voltage during UDDS

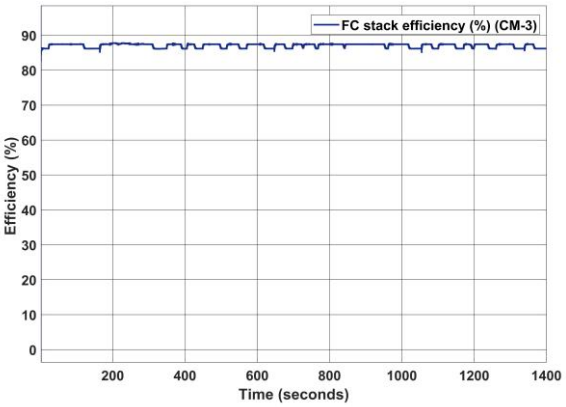

Figure. 15 FC stack efficiency during UDDS

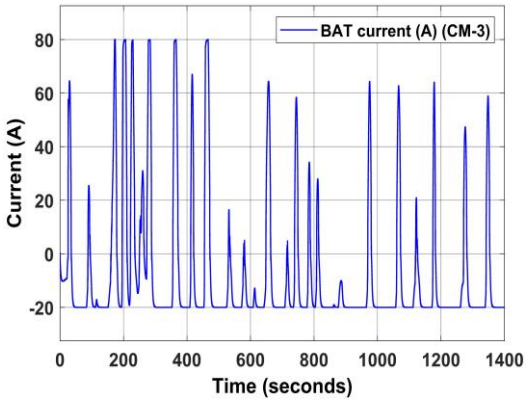

(a)

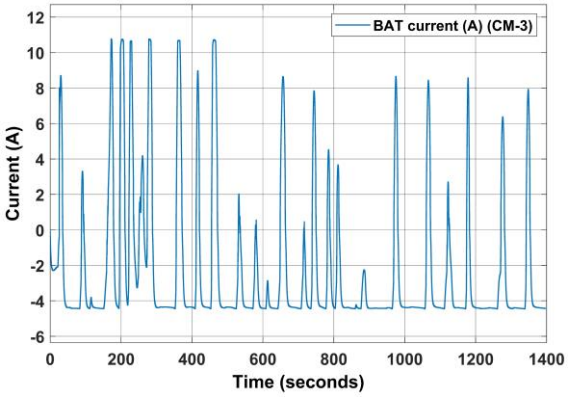

(b)

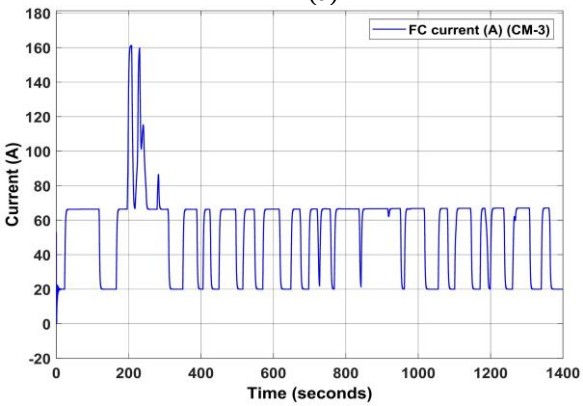

(c)

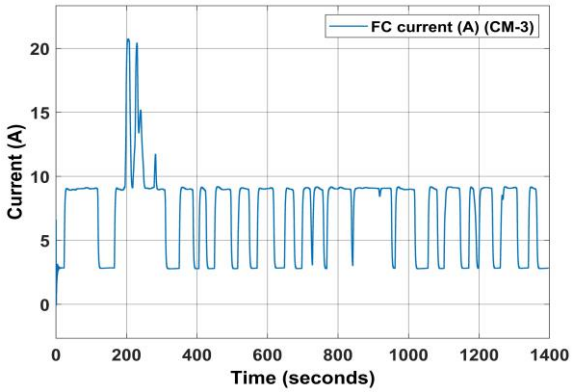

(d)

Figure. 16 Converters input/output currents for BAT (a and b) respectively and for FC (c and d) respectively during UDDS

Table 4. Average FC stack efficiency (%) and mean value of H_2 consumption (lpm) during three drive cycles

CMs	Results of	UDDS
CM-1	Average FC efficiency	86%
	Mean value of H_2 use	23.97 lpm
CM-2	Average FC efficiency	86.42%
	Mean value of H_2 use	23.98 lpm
CM-3	Average FC efficiency	87.4%
	Mean value of H_2 use	23.72 lpm
CMs	Results of	OCC
CM-1	Average FC efficiency	87.2%
	Mean value of H_2 use	22.1 lpm
CM-2	Average FC efficiency	87.24%
	Mean value of H_2 use	22 lpm
CM-3	Average FC efficiency	87.8%
	Mean value of H_2 use	21.23 lpm
CMs	Results of	FTP
CM-1	Average FC efficiency	74%
	Mean value of H_2 use	21.84 lpm
CM-2	Average FC efficiency	78.4%
	Mean value of H_2 use	19.77 lpm
CM-3	Average FC efficiency	86.19%
	Mean value of H_2 use	17.85 lpm

The significant noteworthy that the CM-3 increased the average efficiency of the FC stack by 16.74% over the CM-1 and decreased the amount of hydrogen fuel consumption (lpm) mean value by 22.35% during the FTP driving cycle. Also, the CM-3 maintained the DC-bus voltage during OCC and FTP more than the other proposed control methodologies (CM-1 and CM-2) whereby at OCC the DC-bus by (CM-3) is between 298.5V-311.1V (Mean value is 301.9V), and DC-bus by (CM-1 and CM-2) is between 297.9V-324.3V (Mean value is 304.7V), and between 297.2V-314.2V (Mean value is 302.8V) respectively. And at FTP the DC-bus by (CM-3) is between 299.8V-309.1V (Mean value is 300.2V), and DC-bus by (CM-1 and CM-2) is between 296V-321.6V (Mean value is 307.4V), and between 298.2V-318.2V (Mean value is 302.8V) respectively.

Furthermore, the current of the converters by CM-3 is demonstrated as does not surpass their output rating currents during the highest load demand of all driving cycles as shown in Fig. 16 the converters current during UDDS, where the max input current to converters (BAT is 80A and FC is 161.2A) and the max output current from the converters (BAT is 10.79A and FC is 20.7A).

The results comparison of the simulation among various AI EMS schemes has indicated that CM-3 is the powerful technique for the perfect power flow of the proposed FCHEV with remarkably exceptional improvements compared to other control methodologies (CM-1 and CM-2). Thus, ANNs shows outperform more than FLC over all the driving cycles as well as an excellent performance of RWNN-PI more than WNN-PI. Therefore, the proposed AI EMS and PSO algorithm can be employed by future software developers as a novel artificial intelligence control approach to address the development of emerging technologies in hybrid electric vehicles. Additionally, future work will focus on verification experiments by the proposed CM-3 for AI EMS to compare the simulation results with experimental results.

6. Conclusion

This paper provides an energy management system based on an artificial intelligent controller to manage the power flow of a fuel cell hybrid electric vehicle that integrates three power sources FC, BAT and UC. A comparison of the simulation outcomes is provided among various AI EMS that aimed toward choosing the best control methodology which in return reduces the FCHEV powertrain hydrogen fuel consumption and improves system efficiency. Hence, the proposed AI EMS schemes considered the output characteristics of the power resources, as well as their dynamic responsiveness and restrictions. As a result, the UC is the highest response to load power demand variations during both phases of acceleration and deceleration while the FC system delivers steady-state load power and the BAT provides a medium-frequency component to the load power demand which led to assists the FC to cover the remaining load power required.

The simulation results prove that CM-3 the more effective to satisfy the aim of this study among the others CM-1 and CM-2, especially at OCC and FTP driving cycles. Where CM-3 provides optimum power flow between power sources and load power of FCHEV. As a consequence, the BAT and UC are run in a safe manner and extend their lifetime. Moreover, the average efficiency of the FC stack has been increased, and the amount of hydrogen fuel consumption has been decreased; the duty cycle values of the converters are less than 90%, stable as well as the BAT and FC converter input/output current does not surpass their output rating currents, as a result, the switches of both converters have a longer lifespan. Overall, the CM-3 shows that ANNs and RWNN-PI are reliable in this proposed AI EMS which can be employed over different driving cycles.

Conflicts of interest

The authors declare that we do not have any circumstances or interest that may affect the results discussed in this manuscript.

Author contributions

Conceptualization, Mustafa A. Kamoona and Oday A Ahmed; methodology, Mustafa A. Kamoona; software, Mustafa A. Kamoona and Oday A Ahmed; validation, Mustafa A. Kamoona, Omer Cihan Kivanc, and Oday A Ahmed; formal analysis, Mustafa A. Kamoona; investigation, Omer Cihan Kivanc and Oday A Ahmed; resources, Oday A Ahmed; data curation, Omer Cihan Kivanc; writing—original draft preparation, Mustafa A. Kamoona; writing—review and editing, Omer Cihan Kivanc and Oday A Ahmed; visualization, Omer Cihan Kivanc; supervision, Oday A Ahmed; project administration, Mustafa A. Kamoona and Oday A Ahmed; funding acquisition, Mustafa A. Kamoona.

References

[1] A. Khan and N. Javaid, "Optimal sizing of a stand-alone photovoltaic, wind turbine and fuel cell systems", *Computers & Electrical Engineering*, Vol. 85, pp. 1-20, 2020.

[2] E. A. Grunditz and T. Thiringer, "Performance analysis of current BEVs based on a comprehensive review of specifications", *IEEE Transactions on Transportation Electrification*, Vol. 2, No. 3, pp. 270-289, 2016.

[3] F. U. Noor, S. Padmanaban, L. M. Popa, M. N. Mollah, and E. Hossain, "A comprehensive study of key electric vehicle (EV) components, technologies, challenges, impacts, and future direction of development", *Energies*, Vol. 10, No. 8, pp. 1-84, 2017.

[4] I. G. Jang, C. S. Lee, and S. H. Hwang, "Energy Optimization of Electric Vehicles by Distributing Driving Power Considering System State Changes", *Energies*, Vol. 14, No. 3, pp. 1-238, 2021.

[5] N. Bizon and P. Thounthong, "Real-time strategies to optimize the fueling of the fuel cell hybrid power source: A review of issues, challenges and a new approach", *Renewable and Sustainable Energy Reviews*, Vol. 91, pp. 1089-1102, 2018.

[6] H. S. Das, C. W. Tan, and A. H. M. Yatim, "Fuel cell hybrid electric vehicles: A review on power conditioning units and topologies", *Renewable and Sustainable Energy Reviews*, Vol. 76, pp. 268-291, 2017.

[7] X. Lü, Y. Wu, J. Lian, Y. Zhang, C. Chen, P. Wang, and L. Meng, "Energy management of hybrid electric vehicles: A review of energy optimization of fuel cell hybrid power system based on genetic algorithm", *Energy Conversion and Management*, Vol. 205, pp. 1-26, 2020.

[8] M. Yue, S. Jemei, R. Gouriveau, and N. Zerhouni, "Review on health-conscious energy management strategies for fuel cell hybrid electric vehicles: Degradation models and strategies", *International Journal of Hydrogen Energy*, Vol. 44, No. 13, pp. 6844-6861, 2019.

[9] B. Zhou, J. B. Burl, and A. Rezaei, "Equivalent consumption minimization strategy with consideration of battery aging for parallel hybrid electric vehicles", *IEEE Access*, Vol. 8, pp. 204770-204781, 2020.

[10] C. Du, S. Huang, Y. Jiang, D. Wu, and Y. Li, "Optimization of Energy Management Strategy for Fuel Cell Hybrid Electric Vehicles Based on Dynamic Programming", *Energies*, Vol. 15, No. 12, pp. 1-25, 2022.

[11] Y. Luo, Y. Wu, B. Li, J. Qu, S. P. Feng, and P. K. Chu, "Optimization and cutting-edge design of fuel-cell hybrid electric vehicles", *International Journal of Energy Research*, Vol. 45, No. 13, pp. 18392-18423, 2021.

[12] M. Sellali, A. Ravey, A. Betka, A. Kouzou, M. Benbouzid, A. Djerdir, R. Kennel, and M. Abdelrahem, "Multi-Objective Optimization-Based Health-Conscious Predictive Energy Management Strategy for Fuel Cell Hybrid Electric Vehicles", *Energies*, Vol. 15, No. 4, pp. 1-17, 2022.

[13] M. Yue, Z. A. Masry, S. Jemei, and N. Zerhouni, "An online prognostics-based health management strategy for fuel cell hybrid electric vehicles", *International Journal of Hydrogen Energy*, Vol. 46, No. 24, pp. 13206-13218, 2021.

[14] W. Lee, H. Jeoung, D. Park, T. Kim, H. Lee, and N. Kim, "A real-time intelligent energy management strategy for hybrid electric vehicles using reinforcement learning", *IEEE Access*, Vol. 9, pp. 72759-72768, 2021.

[15] M. Gaber, S. H. E. Banna, M. E. Dabah, and M. S. Hamad, "Intelligent Energy Management System for an all-electric ship based on adaptive neuro-fuzzy inference system", *Energy Reports*, Vol. 7, pp. 7989-7998, 2021.

[16] M. Suhail, I. Akhtar, S. Kirmani, and M. Jameel, "Development of progressive fuzzy logic and ANFIS control for energy management of plug-in hybrid electric vehicle",

Ieee Access, Vol. 9, pp. 62219-62231, 2021.

[17] F. Tao, L. Zhu, Z. Fu, P. Si, and L. Sun, "Frequency decoupling-based energy management strategy for fuel cell/battery/ultracapacitor hybrid vehicle using fuzzy control method", *IEEE Access*, Vol. 8, pp. 166491-166502, 2020.

[18] Wang, Jianlin, J. Zhou, and D. Xu, "A real-time predictive energy management strategy of fuel cell/battery/ultra-capacitor hybrid energy storage system in electric vehicle", In: *Proc. of 2020 Chinese Automation Congress (CAC) IEEE*, pp. 3951-3954. 2020.

[19] O. A. Ahmed, "Investigation into high efficiency DC-DC converter topologies for a DC microgrid system", *PhD Diss, University of Leicester*, pp. 1-322, 2011.

[20] Maxwell Boostcap®BCAP1200 UC Datasheet, Available online: https://www.datasheetarchive.com/pdf/download.php?id=692d2c8a33a1c020f38f0ee5addb244b9a3475&type=M&term=BCAP1200, *last accessed*, 2022/07/21.

[21] U-Charge U1-12XP Lithium-ion Battery Datasheet, Available online: https://www.celltech.se/fileadmin/user_upload/Celltech/Products/Litium_laddningsbara/Valence_Modules/XP_Module_Datasheet.pdf (Accessed, 2022/07/21).

[22] HyPM-HD12 PEMFC Datasheet, Available online: https://silo.tips/download/hypm-fuel-cell-power-modules, *last accessed*, 2022/07/21.

[23] A. A. Obed, A. L. Saleh, and A. K. Kadhim, "Speed performance evaluation of BLDC motor based on dynamic wavelet neural network and PSO algorithm", *International Journal of Power Electronics and Drive Systems*, Vol. 10, No. 4, pp. 1742-1750, 2019.